



Relative quantification of sulfenic acids in plasma proteins using differential labelling and mass spectrometry coupled with 473 nm photo-dissociation analysis: A multiplexed approach applied to an Alzheimer's disease cohort

Jean-Valery Guillaubez, Delphine Pitrat, Yann Bretonnière, Jérôme Lemoine, Marion Girod

► To cite this version:

Jean-Valery Guillaubez, Delphine Pitrat, Yann Bretonnière, Jérôme Lemoine, Marion Girod. Relative quantification of sulfenic acids in plasma proteins using differential labelling and mass spectrometry coupled with 473 nm photo-dissociation analysis: A multiplexed approach applied to an Alzheimer's disease cohort. *Talanta*, 2022, 250, pp.123745. 10.1016/j.talanta.2022.123745 . hal-03740463

HAL Id: hal-03740463

<https://hal.science/hal-03740463>

Submitted on 29 Jul 2022

HAL is a multi-disciplinary open access archive for the deposit and dissemination of scientific research documents, whether they are published or not. The documents may come from teaching and research institutions in France or abroad, or from public or private research centers.

L'archive ouverte pluridisciplinaire **HAL**, est destinée au dépôt et à la diffusion de documents scientifiques de niveau recherche, publiés ou non, émanant des établissements d'enseignement et de recherche français ou étrangers, des laboratoires publics ou privés.

Relative quantification of sulfenic acids in plasma proteins using differential labelling and mass spectrometry coupled with 473 nm photo-dissociation analysis: a multiplexed approach applied to an Alzheimer's disease cohort

**Jean-Valery Guillaubez¹, Delphine Pitrat², Yann Bretonnière², Jérôme Lemoine¹,
Marion Girod¹**

¹ Institut des Sciences Analytiques, UMR 5280, Université Lyon 1, CNRS, Villeurbanne.

² Laboratoire de Chimie ENS Lyon, UMR 5582, ENS Lyon CNRS et Université Lyon 1, France

Corresponding author: Marion Girod, Email : marion.girod@univ-lyon1.fr

Abstract

Cysteine (Cys) is subject to a variety of reversible post-translational modifications such as formation of sulfenic acid (Cys-SOH). If this modification is often involved in normal biological activities, it can also be the result of oxidative damage. Indeed, oxidative stress yields abnormal cysteine oxidations that affect protein function and structure and can lead to neurodegenerative diseases. In a context of population ageing, validation of novel biomarkers for detection of neurodegenerative diseases is important. However, Cys-SOH proteins investigation in large human cohorts is challenging due to their low abundance and lability under endogenous conditions. To improve the detection specificity towards the oxidized protein subpopulation, we developed a method that makes use of a mass spectrometer coupled with visible laser induced dissociation (LID) to add a stringent optical specificity to the mass selectivity. Since peptides do not naturally absorb in the visible range, this approach relies on the proper chemical derivatization of Cys-SOH with a chromophore functionalized with a cyclohexanedione. To compensate for the significant variability in total protein expression within the samples and any experimental bias, a normalizing strategy using free thiol (Cys-SH) cysteine peptides derivatized with a maleimide chromophore as internal references was used. Thanks to the differential tagging, oxidative ratios were then obtained for 69 Cys-containing peptides from 19 proteins tracked by parallel reaction monitoring (PRM) LID, in a cohort of 49 human plasma samples from Alzheimer disease (AD) patients. A statistical analysis indicated that, for the proteins monitored, the Cys oxidative ratio does not correlate with the diagnosis of AD. Nevertheless, the PRM-LID method allows the unbiased, sensitive and robust relative quantification of Cys oxidation within cohorts of samples.

Keywords

Differential chromophore derivatization, cysteine oxidation, laser induced dissociation, mass spectrometry

INTRODUCTION

Since their discovery in living organisms, reactive oxygen species (ROS) have been the subject of extensive research on their involvement in cellular dysfunction and pathologies. Indeed, the accumulation of ROS affects the redox balance of cell, leading to oxidative stress. The oxidative damages caused by oxidative stress are numerous, can affect different biomolecules (DNA, proteins, or lipids), and are closely linked to the development and progression of a multitude of pathologies such as neurodegenerative diseases [1–4]. These types of diseases are characterized by progressive loss of function or apoptosis of neuronal cells. Mitochondrial DNA damage, peroxidation of fatty acids and dysfunctions of enzymes such as glutathione transferases (for elimination of ROS) are a few examples of the involvement of oxidative stress in neurodegenerative diseases such as Alzheimer's disease (AD) and Parkinson's disease [1,5]. The lack of ROS regulation also results in an increase of oxidative modifications on proteins. One of the natural amino acids most susceptible to oxidative modification is cysteine (Cys) due to the high reactivity of the thiol group [6,7]. Common reversible oxidation of Cys by ROS include formation of sulfenic acid (SOH) or disulfide bonds [8], before irreversible oxidation into sulfinic acid (SO₂H) and sulfonic acid (SO₃H). Processes of oxidation are still difficult to access, because of their low stoichiometry. Indeed, oxidized Cys sites concentration in human plasma range from 0.4 to 1.0 nmol/mg protein [9]. Though, this reversible oxidation into SOH of cysteine residues has been shown to be involved in redox homeostasis, cellular signaling, enzymatic catalysis and structural stability [10].

Therefore, this reversible oxidative modification might be used as biomarkers of protein oxidation level, a measurement of particular interest for the assessment of AD given the importance of oxidative stress in neurodegenerative diseases. However, validation of such

low concentrated biomarkers for clinical applications is still critical. This relative failure result firstly of a high rate of false positives during the discovery phase deployed for the identification of biomarker candidates, particularly because of the high complexity and dynamic range concentration of the samples to be analyzed. On the other hand, the accurate and sensitive quantification of proteins and peptides in complex matrices such as plasma, serum or urine at high throughput is currently a key issue for clinical evaluation of candidate biomarkers.

The evidence of the key role of Cys in mediating signal transduction processes and gene expression has led to successive developments of biochemical and analytical methods aimed at characterizing the redox state of Cys [6]. The complexity of cysteine chemistry and modifications goes hand in hand with the breadth of methods currently available for their characterization. Affinity- or fluorescence- based methods allow a global qualitative detection of the amount of oxidized proteins after specific tagging of reduced Cys [9,11–13]. Liquid chromatography (LC) coupled to tandem mass spectrometry-based (MS/MS) methodologies have been developed in order to have access on the extent of oxidative damage and their localization for each specific protein present in complex cellular extracts or biofluids. Differential labeling is the most widely used approach, allowing to distinguish reduced and oxidized Cys by their mass. In differential labeling, the initially reduced Cys are first blocked by an alkylating reagent such as N-ethylmaleimide or iodoacetamide. Oxidized Cys are then reduced with arsenite or Tris(2-carboxyethyl)phosphine (TCEP) and alkylated with a second thiol labelling probe. Isotope coded affinity tags (ICAT) containing an iodoacetyl group, a cleavable biotin tag and a linker which exists in isotopically light and heavy forms were specifically designed for differential labeling of free vs. oxidized Cys residues [14–16]. Recently, a new type of tandem mass tags (TMT) specific to thiols

containing a iodoacetyl group has been developed for the study of cysteine oxidation [17,18]. Different isobaric iodoTMT reagents, yielding different reporter ions upon collisional activation, are used to differentially tag reduced and oxidized cysteine. Relative quantification is achieved either using the isotope coded tags or in tandem MS via reporter ion intensity comparison. In each case, the signal of the Cys-oxidized peptides is normalized by the total amount of free Cys peptides. Alternatively, it is also possible to introduce a specific reacting agent, such as dimedone derivatives, to directly tag the Cys-SOH [19]. However, unless enrichment step of the sub-population of oxidized proteins on avidin or antiTMT columns, access to the lowest limit of quantification (LOQ) is difficult to achieve with collision-induced dissociation (CID) due to the huge dynamic range of protein concentrations in biological extracts and the great complexity of trypsin hydrolysates.

Detection specificity toward a subset of targeted peptides can be obtained by substituting the classical CID mode by laser induced dissociation (LID). Infrared multiphoton photodissociation (IRMPD) at 10.6 μm has shown interesting propensity to differentiate phospho- and non-phosphorylated peptides [20] due to increased photon absorption of the phosphate group. The fragmentation specificity of peptides has been similarly illustrated in the ultraviolet range (UVPD) by leveraging natural absorption of intrinsic chromophores such as disulfide bonds or tyrosine residue [21,22]. Nonetheless, the most obvious rationale to introduce fragmentation specificity lies in targeting only the subset of peptides after grafting them with a proper chromophore [23,24]. Photodissociation at 351 nm UVPD [25] or in the visible range at 473 nm [26–28] allowed to photo-fragment only the Cys-peptides selectively tagged with specific chromophores and pinpoint them from complex biological samples on the basis of the appearance of a photo-induced reporter ion and extensive series of b and y fragment ions.

Here, we report the relative quantification of total protein cysteine oxidative ratios by liquid chromatography coupled to LID-MS in a cohort of plasma samples. Multiplexed targeted LID parallel reaction monitoring (PRM) strategy was developed to monitor Dabcyl cyclohexanedione derivatized Cys-SOH peptides of human plasma proteins after trypsin digestion. Because of the natural variability in total protein expression within samples and possible instrumental bias, a differential tagging approach was proposed. Indeed, the signal of each Cys-SOH peptides was normalized by the corresponding Cys-SH peptide identified *via* the derivatization of free thiol with a Dabcyl maleimide chromophore. Quality control samples were introduced throughout the clinical cohort study, in order to assess the overall performance of the method and ensure the validity of statistical comparisons between healthy controls and AD patients groups.

EXPERIMENTAL SECTION

Chemicals and reagents

Optima® LC-MS Grade water (H₂O), methanol (MeOH) and acetonitrile (ACN) were obtained from Fisher Chemical, dimethyl sulfoxide (DMSO) from Sigma-Aldrich and LC-MS Grade formic acid (F.A) from Fluka. DL-Dithiothreitol (DTT), Iodoacetamide (IAM), Ammonium Bicarbonate (AMBIC), trypsin from porcine pancreas were purchased from Sigma-Aldrich. Dabcyl cyclohexanedione chromophore was designed and synthesized as described previously [29]. The Dabcyl C2 maleimide chromophore was purchased from Eurogentec (Belgium).

Standard Protocol Approvals, Registrations and Patient Consents

The cohort included 49 patients between 60 and 75 years old: 15 healthy controls and 34 patients with a diagnosis of AD stage 2. All patients underwent a thorough clinical examination including biological laboratory tests, neuropsychological assessments, and brain imaging. They all gave written informed consent for participation in this study. The samples were acquired from the CRB-CHUM platform of the Montpellier University Hospital (<http://www.chu-montpellier.fr>; collection manager: Professor Sylvain LEHMANN s-lehmann@chu-montpellier.fr) through the BIOBANKS identifier - BB-0033-00031.

Sample preparation

For the derivatization of endogenous oxidized and free cysteine in plasma samples, 10 μ L of human plasma were mixed with 5.5 μ L of dithiothreitol (DTT) at 150 mM in ammonium bicarbonate (AMBIC) 50 mM and 184.5 μ L of H₂O then denaturated at 60°C for 40 min. Samples were cooled at room temperature, diluted with 300 μ L of H₂O, then 250 μ L of 2.12 mM DabDn in DMSO were added. The protein digestion was performed in parallel with 10 μ L of a 5 mg/mL trypsin solution, to reach a 33 % organic/aqueous phase ratio. The samples were then left reacting at 37°C during 8 h. 5.5 μ L of DTT were added to the samples to reduce reformed disulfide bridges during 15 minutes, followed by cysteine thiol derivatization with 250 μ L DabMal 5.3 mM in DMSO and 500 μ L of H₂O reacting overnight (14 h). Samples were purified on Oasis HLB 6cc cartridge and eluted with 1.5 mL of MeOH + 0.5 % F.A. Eluted samples were dried at RT under N₂ stream and resuspended in 200 μ L of a H₂O/ACN 75/25 + 0.1 % F.A solution. A schematic workflow of the sample preparation can be found Scheme S1 in the Supplementary Material.

HPLC separation

Liquid chromatography was performed with a Thermo Scientific Dionex UltiMate 3000 pump and autosampler system using a Waters XBridge Peptide C18 column (2.1 mm, 3.5 μ M), and H₂O+0.1 % F.A (eluent A) and ACN+0.1 % F.A (eluent B) as mobile phases at 300 μ L/min. 10 μ L of each sample were injected.

HPLC separation of the derivatized endogenous Cys-SOH and Cys-SH peptides in plasma samples consists of a linear gradient from 5 % to 48 % of eluent B for 60 min. After a washing step at 100 % of B for 10 min, the gradient was returned to the initial conditions and the column was re-equilibrated for 10 min.

Instrumentation and mass spectrometry operating conditions

Experiments were performed on a modified hybrid quadrupole-orbitrap QExactive® mass spectrometer (Thermo Fisher Scientific, San Jose, CA, USA) equipped with a HESI ion source. This instrument has been modified to allow visible laser irradiation of ions by fitting a silica window on the rear of the HCD (Higher-energy Collisional Dissociation) cell [28]. The laser is a 473 nm continuous wavelength laser (ACAL BFI, Evry, France), permanently turned on with an output power of 800 mW. Electrospray ionization in HESI source was achieved on positive mode with a spray voltage of 4 kV at 320°C, and sheath gas and auxiliary gas flow rates were 12 and 4 (arbitrary unit), respectively. The AGC target was set to 1e6, pairing with a maximum injection time at 100 ms, and the S-Lens RF level set to 55 (arb. unit). Resolution in the orbitrap analyzer was set to 35,000 during PRM analysis. For MS/MS analysis, isolation of the precursor was defined with a ± 1.0 m/z window in order to select isotopic patterns. PRM list of precursors is available in the Supplementary Material (Table S1). For LID fragmentation, the activation time was set to 25 ms and an activation energy of 3 eV applied in order to avoid CID contaminating events. For data-dependent top 10 experiments, the full

MS scans were done over a m/z 300-1500 range with a resolution of 35 000. For the data-dependent MS/MS scans, the resolution was set at 17 500, isolation 2 m/z , with a normalized collision energy of 28 (arbitrary unit). To exclude the redundant processing of dominant ions and allow selection of low abundant oxidized peptides, a dynamic exclusion time of 20 s was set.

Peptide and Protein Identification and Quantification

Peptide identification and quantification from the PRM-LID analysis is performed using Skyline [30]. First, the most intense protonated precursor ion from $z=2$ to 5 is selected and all fragment ions assigned (mass errors <10 ppm are checked using XCalibur software in order to confirm the identification). Then, the most appropriate fragment ions are selected for the quantification according to the following rules: the fragment must be i) specific of the monitored peptide and with a large peptide sequence coverage (i.e. no low (1 and 2) b and y fragments). Fragments presenting a dabcyI group loss (251.1 Da) are extremely specific of derivatized peptide and LID fragmentation and are usually preferred, ii) not interfered, iii) intense enough to allow robust quantification and iv) limited to 3 ions for low mass peptide (<20 AA) and 4 ions for higher mass peptides (>20 AA). The precursor ion is also summed for the quantification of the peptide (only if not interfered), as well as its first isotopic ion, in order to compensate a potential shift of laser power during analysis. Chromatographic peaks corresponding to fragment ions and precursor of the DabMal and DabDn derivatized peptides are integrated and their areas respectively summed with Skyline, then exported for calculation of the oxidative ratios.

Fragmentation spectra from top10 analysis were converted to peaklists using PAVA RawRead and searched against sequences of Human proteins contained in the Swissprot human database (downloaded 2021.06.18) using Protein Prospector [31]. All searches used the following parameters: mass tolerances in MS and MS/MS modes were 15 ppm and 0.02 Daltons, respectively. Trypsin was designated as the enzyme and no missed cleavage was allowed. To search for derivatized peptides, user defined variable modifications of +419.1846 Da and +391.1644 Da, corresponding to the exact masses of Cys-SOH labeled with DabDn and Cys-SH labeled with DabMal on, respectively. The methionine oxidation variable modification was also considered. The maximum expected value allowed was set at up to 0.01 (protein) and 0.05 (peptide).

RESULTS AND DISCUSSION

The primary objective of the study was to develop a PRM-LID MS-based assay to characterize the total oxidative ratio of plasma proteins in a cohort of AD patients. Studies have focused on PRM compatibility with complex proteomic analysis, comparing QqQ triple quadrupoles and high resolution (HRMS) instruments on target analysis (MRM and PRM, respectively). These studies ensure that performance of HRMS instrument is comparable to QqQ on linearity, specificity, selectivity and sensibility thanks to HR spectra. Then, PRM analysis is suitable for proteomics analysis over complex biological samples in large cohorts [32–34]. For an increased sensitivity, the Cys-SOH peptides were specifically derivatized with a Dabcyl cyclohexanedione (DabDn) to be specifically detected by LID [29]. In order to mitigate the significant variability in total protein expression within the samples and possible bias of the

Cys-SOH derivatization, Cys-SH corresponding peptides, derivatized with a Dabcyl maleimide chromophore (DabMal) [35] were used as internal references in a differential tagging approach.

Reduction protocol of plasma samples and differential chromophore derivatizations

A special care has been taken to the protein reduction step during the sample preparation in order to access the Cys-SH released from S-S bridges but not from reduced endogenous Cys-SOH. We thus checked the relative signal of derivatized endogenous Cys-SOH peptides obtained by PRM-LID for 7 concentrated proteins [29] from plasma samples prepared with 3 different cysteine-DTT ratios: 1-0.3, 1-3 and 1-30 before the derivatization with the DabDn. The nature of the reducing agent was also evaluated using TCEP with a 1-3 ratio. Figure 1 shows the relative amount of oxidized proteins between the different sample preparation conditions. The relative amount of endogenous oxidized protein was calculated by averaging the signal value of each individual derivatized Cys-SOH peptide of the same protein.

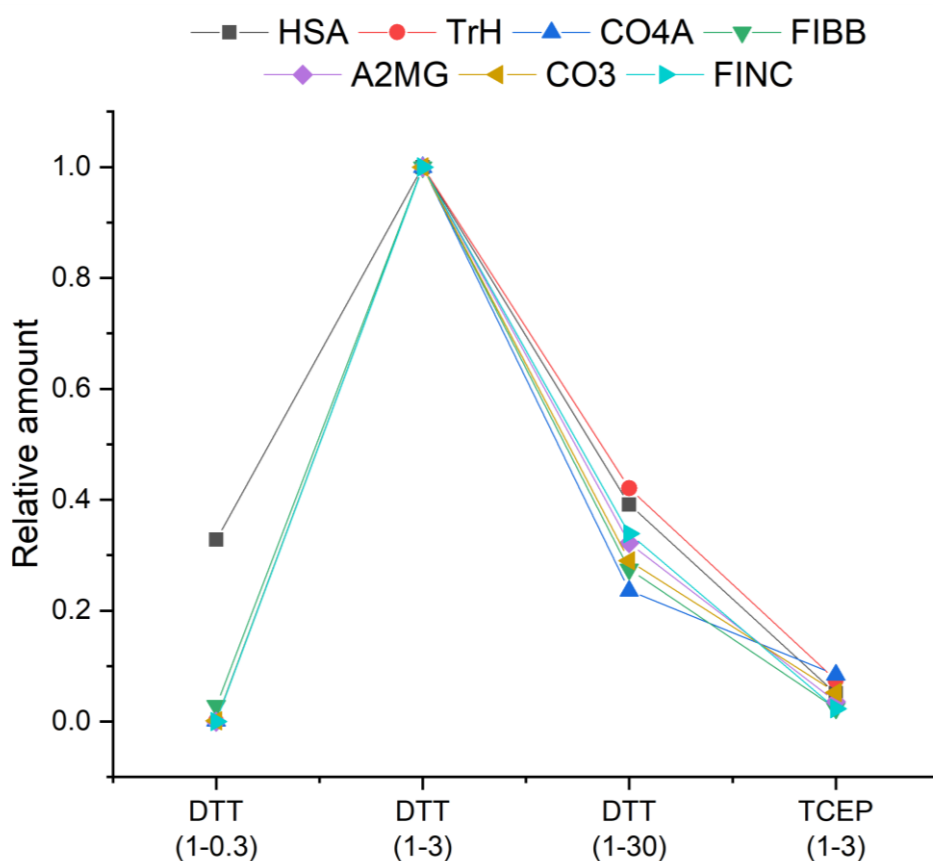


Figure 1: Relative quantification of oxidized proteins obtained by PRM-LID between the different sample preparation conditions: cysteine-DTT ratio 1-0.3; 1-3 and 1-30 and cysteine-TCEP ratio 1-3. Normalization was made for each protein by dividing its mean signal intensity by the maximal signal intensity between the 4 conditions.

The use of 1-0.3 and 1-30 cysteine-DTT ratios lead to a significant decrease of the amount of derivatized Cys-SOH for all proteins, compare to the 1-3 ratio. With a high amount of DTT (1-30 ratio), the endogenous Cys-SOH were probably reduced and not derivatized/detected any longer. For the 1-0.3 cysteine-DTT ratio, reduction of the disulfide bridges would not be complete, which prevented proteins digestion as well as access to oxidized cysteine by the chromophore. As agreed with the literature, the use of TCEP resulted in the reduction of

sulfenic acid since a very small amount of endogenous derivatized Cys-SOH was detected among all the monitored proteins. Thus, to preserve the Cys-SOH and enhance the protein digestion, a cysteine-DTT ratio of 1-3 has been used to reduce disulfide bridges.

Then, the conditions of Cys-SH peptide derivatization with the Dabcyl maleimide, previously described [26,28], have been adapted for our protocol of differential tagging. Indeed, TCEP was used as reducing agent before chromophore derivatization, which was not compatible with the analysis of Cys-SOH peptides, as reported above. Thus, the samples were sequentially derivatized: protein Cys-SOH were first tagged with the DabDn and simultaneously digested with trypsin during 8h, then the DabMal was grafted on the Cys-SH peptides without TCEP for 14h. Although the DabDn and DabMal chromophores are both very strongly non-polar and insoluble in water, their chemical properties are sufficiently different to allow their separation by reverse phase chromatography as well as the separation of the two classes of derivatized peptides. As an example, a chromatogram of the separation of 15 couples of derivatized DabMal Cys-SH and DabDn Cys-SOH peptides is presented in Figure 2.

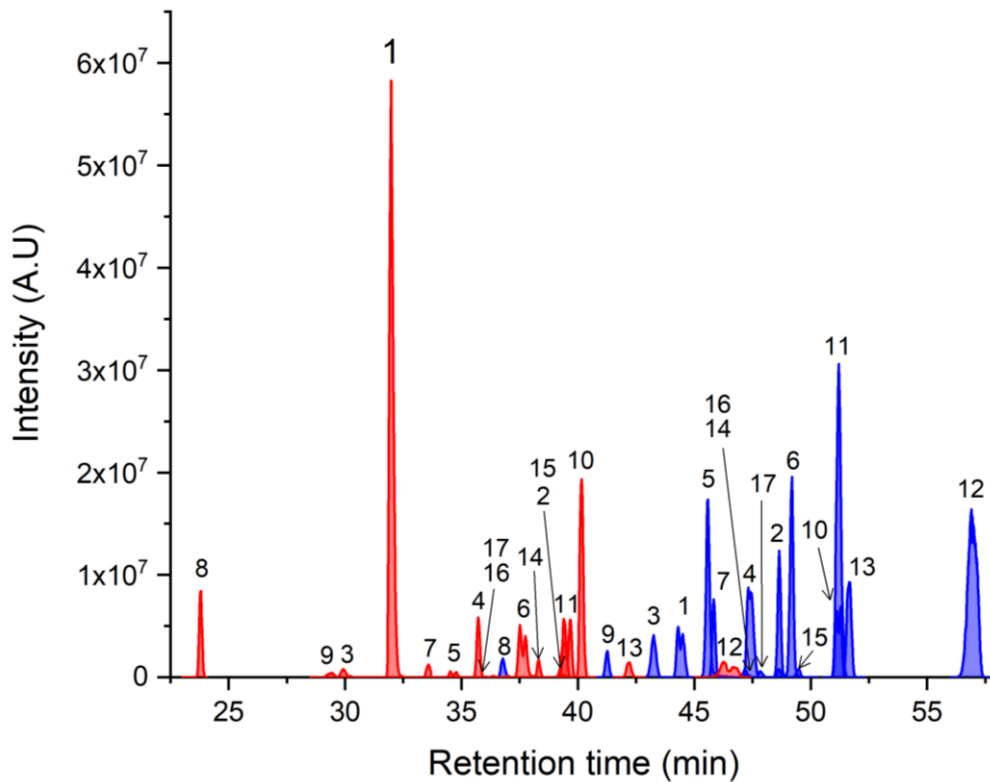


Figure 2: Reconstructed chromatogram of the separation of 15 DabMal derivatized Cys-SH (red) and DabDn derivatized Cys-SOH (blue) peptides from a plasma sample analyzed by PRM-LID. 1- [TrH] WCAVSEHEATK, 2- [TransfH] FDEFFSAGCAPGSK, 3- [CO4A/B] NNVPCSPK, 4- [CO3] DSCVGLVVK, 5- [A2MG] VTAAPQSVCALR, 6- [FIBB] LESDVSAQMEYCR, 7- [FINC] ISCTIANR8- [FIBA] HQSACK, 9- [CERU] TYCSEPEK, 10- [HEMO] DYFMPCPGR, 11- [HPT] VMPICLPSK, 12- [IGCK] SGTASVVCLNNFYPR, 13- [CFAH] SCDIPVFMNAR, 14- [FETUA] EHAVEGDCDFQLLK, 15- [AACT] DEELSCTVVELK, 16- [APOE] LGADMEDVCGR, 17- [CXCL7] ICLDPDAPR. The intensities of the precursor ion and four specific fragment ions were summed for each peptide.

The DabMal derivatized Cys-SH peptides are mainly eluted before the DabDn derivatized Cys-SOH peptides. The average retention time difference between the DabMal derivatized

Cys-SH and the DabDn derivatized Cys-SOH peptides is 10.6 min, which corresponds to a difference of 7.1% of acetonitrile in the mobile phase with our LC gradient. This difference will only induce slightly different ionization efficiency, which is not problematic for relative quantification. Moreover, the retention time distribution of the two classes of derivatized peptides along the chromatogram allows targeting both derivatized Cys-SH and Cys-SOH peptides without significant increase of the duty cycle although the number of selected precursors is doubled. The LID fragmentation of the SVIPSDGPSVACVK peptide with either the Cys-SH derivatized with DabMal or the Cys-SOH derivatized with DabDn are compared in Figure 3 a) and b). LID fragmentation spectra of SVIPSDGPSVAC^{Mal}VK and SVIPSDGPSVAC^{*Dn}VK peptides are very similar, yielding predominantly γ ions and small b ions. Specific ions at m/z 148.08 and 252.11 from the internal fragmentation of dabcyI moiety are also observed for both derivatized peptides [35]. Cys-containing fragment ions mainly present either the loss of the dabcyI group ($[\gamma_7-251.1]^+$ to $[\gamma_{12}-251.1]^+$ on Figure 3) or the loss of the entire chromophore ($[\gamma_4-S(DabMal/Dn)]^+$, $[\gamma_8-S(DabMal/Dn)]^+$). Water loss is also observed from γ ions ($[\gamma_8-H_2O]^+$ to $[\gamma_{11}-H_2O]^+$). The fragment ions $[\gamma_8-269.1]^+$ and $[\gamma_{10}-269.1]^+$, produced by elimination of the dabcyI group at the ester function, are only observed for the SVIPSDGPSVAC^{*Dn}VK peptide (Figure 3a) since it is specific of the cyclohexanedione moiety (Scheme S2).

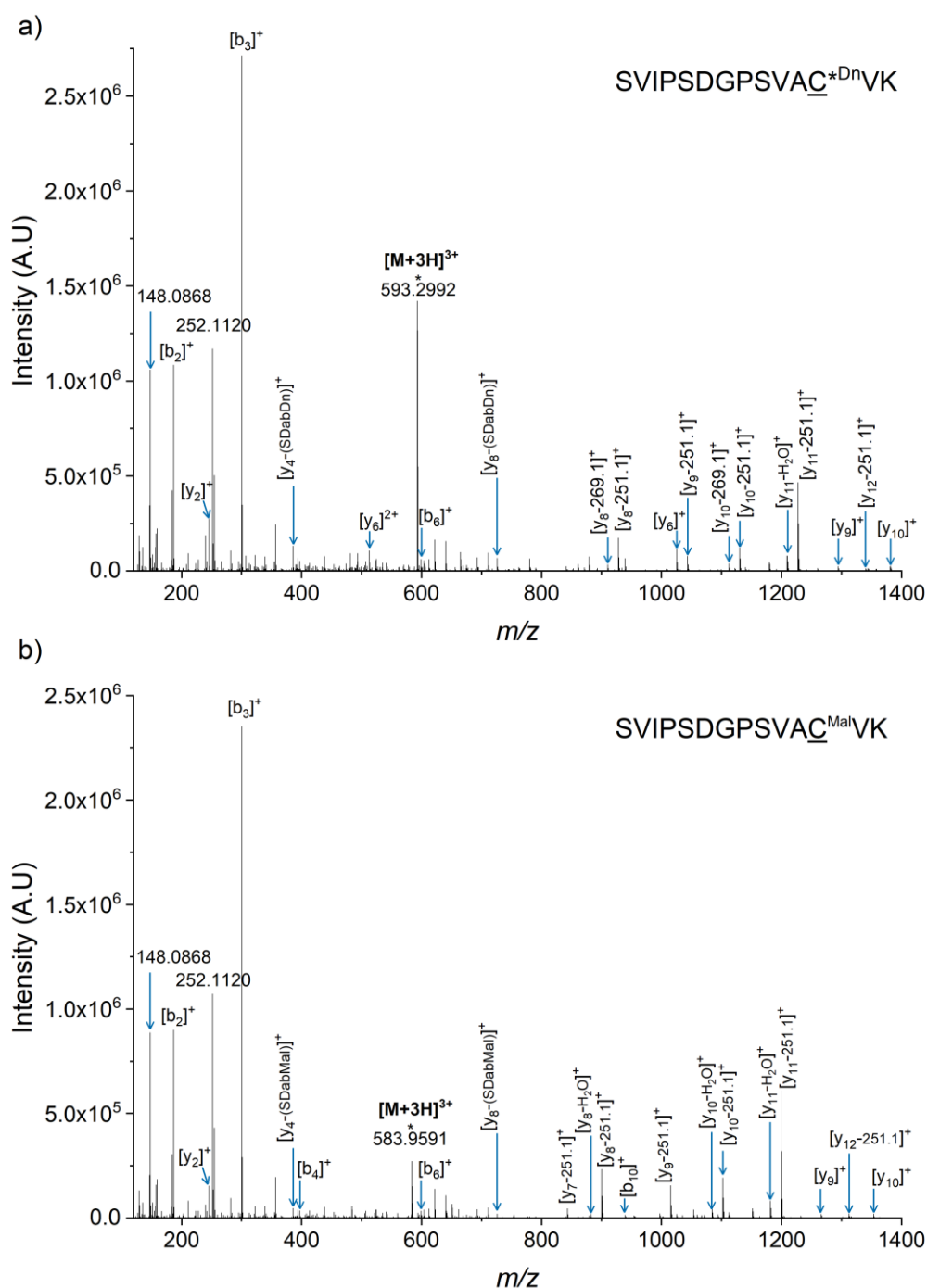


Figure 3: LID spectra of the triply protonated $[M+3H]^{3+}$ a) Cys-SH DabMal derivatized SVIPSDGPSVAC^{Ma}IVK and b) Cys-SOH DabDn derivatized SVIPSDGPSVAC^{*Dn}MaIVK peptides at 473 nm. Irradiation during 25 ms with 800 mW laser power.

The detection and quantification via fragmentation by PRM-LID of both endogenous Cys-SH and Cys-SOH forms of the same peptide derivatized with DabMal and DabDn, respectively, will allow internal normalization of the signals by calculating an oxidative ratio.

Cohort analysis and Quality Control samples

Non-targeted top10 analysis of the cohort plasmas sequentially derivatized with DabDn and DabMal chromophores were first performed in order to define, for future analysis by PRM-LID, a list of Cys-SOH proteins potentially involved in the development processes of Alzheimer's disease. The top10 analysis of the 49 samples allow to detect endogenous derivatized Cys-SOH peptides from 21 to 54 different proteins within the same sample. A global list of these proteins is presented in Table S2 in Supplementary Material. In order to rationalize the PRM-LID analysis in term of duty cycle, a short list of the 18 most intense proteins with retention times distributed along the chromatographic separation has been prepared. These proteins were digested *in silico* and peptides containing one unique cysteine were targeted. Among these peptides, which also contain a methionine, only those for which the non-oxidized methionine form was detected in the top10 analysis of plasma samples were considered. This is meant to prevent interference of methionine oxidation on the Cys-SOH quantification, even if we have shown that the oxidized methionine were not reactive with the DabDn chromophore [29]. In addition, the cysteine containing LGADMEDVCGR peptide of Apolipoprotein E (ApoE) has been included in the PRM-LID method since ApoE, and especially the ApoE4 allele, has been identified as the main genetic risk factor for AD [36]. Moreover, above normal total ApoE and ApoE4 levels in the plasma of AD patients have been reported [37]. Therefore, it could constitute a potential biomarker of

AD. Thus, in total with the internal references, 75 couples of derivatized Cys-SOH and Cys-SH peptides representative of 19 proteins were followed in PRM-LID (Table S1).

The cohort samples were then randomized before analysis by PRM-LID for oxidative ratio measurements. Twelve quality control (QCs) from a random sample were also sequentially derivatized and analyzed with the cohort. The area of the derivatized Cys-SOH (i.e. sum of the precursor ion and 3 to 4 specific fragment ions) was divided by the area of the analogous derivatized Cys-SH peptide to yield the oxidative ratio. Only 69 oxidative ratios could be established from the analysis of the 75 couples of derivatized peptides due absence of detection. The mean oxidative ratios, standard deviations and coefficients of variation were calculated for each peptide in the 12 QC samples run throughout the clinical cohort study (see Table S3 in SI). Figure 4 illustrates the mean oxidative ratio and mean \pm standard deviation values of four targeted peptides in QC samples. The statistical analysis of the 12 QCs showed CVs of oxidative ratios below 20% for all the targeted peptides. 19 of the 69 peptide oxidative ratios (27.5 %) displayed a CV between 10 and 20 %. 20.3 % of the peptides presented oxidative ratios with an excellent CV below 5 %, while the other 52.2 % with a CV between 5 and 10 % (table S3). These results indicated that sample preparation and PRM-LID analysis are suitable for analysis of complex biological cohort samples.

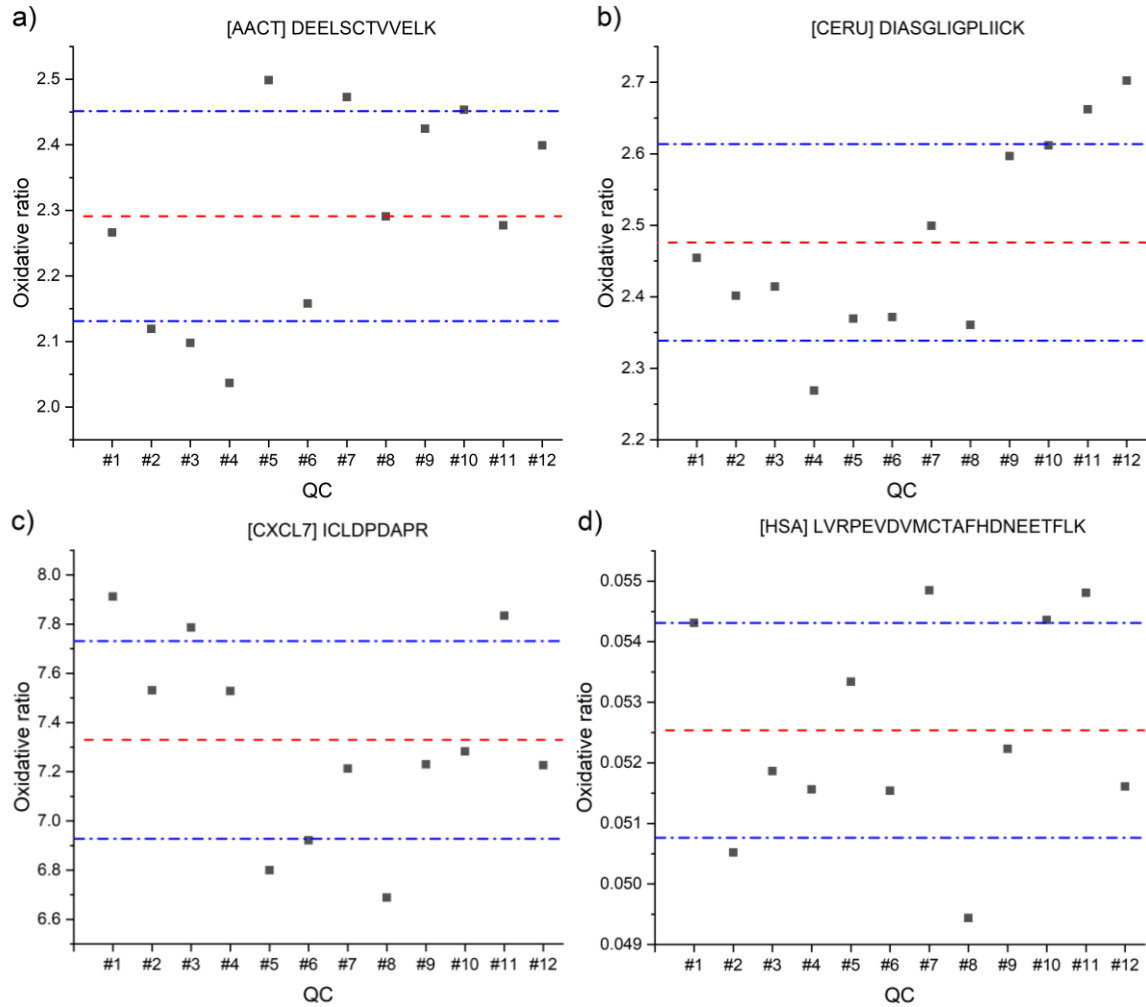


Figure 4: Oxidative ratios for peptides a) DEELSCTVVELK of the [AACT] protein, b) DIASGLIGPLIICK of the [CERU] protein, c) ICLDPDAPR of the [CXCL7] protein and d) LCRPEVDVMCTAFHDNEETFLK of the [HSA] protein in the 12 QC samples. The dotted red line represents the mean oxidative ratio for the 12 QC samples and the blue lines the mean value ± 1 SD. Oxidative ratio was calculated by dividing the area of the derivatized Cys-SOH peptide (i.e. sum of the precursor ion and 3-4 specific fragment ions) by the analogous derivatized Cys-SH peptide.

The peptide oxidative levels were determined for each sample and compared within the cohort. Normalization of the Cys-SOH peptide signal with the analogous Cys-SH peptide allowed to circumvent the differences in protein expression between patients as well as the instrumental variability, as illustrated for 2 peptides in Figure S1 in SI. The absolute signal of the derivatized Cys-SOH peptides was largely dispersed compared with the oxidative ratio within the cohort samples. From the 75 tracked peptides, it appeared that oxidative ratios of the DEELSCTVVELK peptide of the AACT protein and the ICLDPDAPR peptide of the CXCL7 protein were different in some AD samples of the cohort. α -1-antichymotrypsin protein (AACT or SERPINA3) is an acute-phase glycoprotein [38] of approximately 48 kDa, which belongs to the class of serine protease inhibitors. Its production, in the liver or directly in the lungs, is highly stimulated by different cytokines (IL-1 β , TNF- α , IL-6) during inflammation [39]. In addition to being a marker of inflammation, AACT protein has been reported to be responsible for phosphorylation of the Tau protein involved in Alzheimer's disease [40,41]. The protein CXCL7 (Chemokine C-X-C motif ligand 7 or Platelet Basic Protein) is a small protein (approx. 14 kDa) released in large quantities by blood platelets during activation and involved in inflammation, tissue lesions and infections [42]. This protein is usually found in plasma following a defect in blood platelet centrifugation. The oxidative ratio of DEELSCTVVELK peptide of the AACT protein (Figure 5a) was higher than the others for 5 samples from patients with AD (samples 4, 43, 46, 47, 49). This increase of oxidative ratios is not observed for the other targeted peptides in these samples, indicating the absence of sample bias in these results. The ICLDPDAPR peptide of the CXCL7 protein presented a higher oxidative ratio (i.e. a higher level of endogenous Cys-SOH) for 3 AD samples of the cohort (samples 22, 24, 49 Figure 5b). Due to the low incidence of these increases, it is

difficult to conclude on potential use of these peptides as biomarkers specific to Alzheimer's disease.

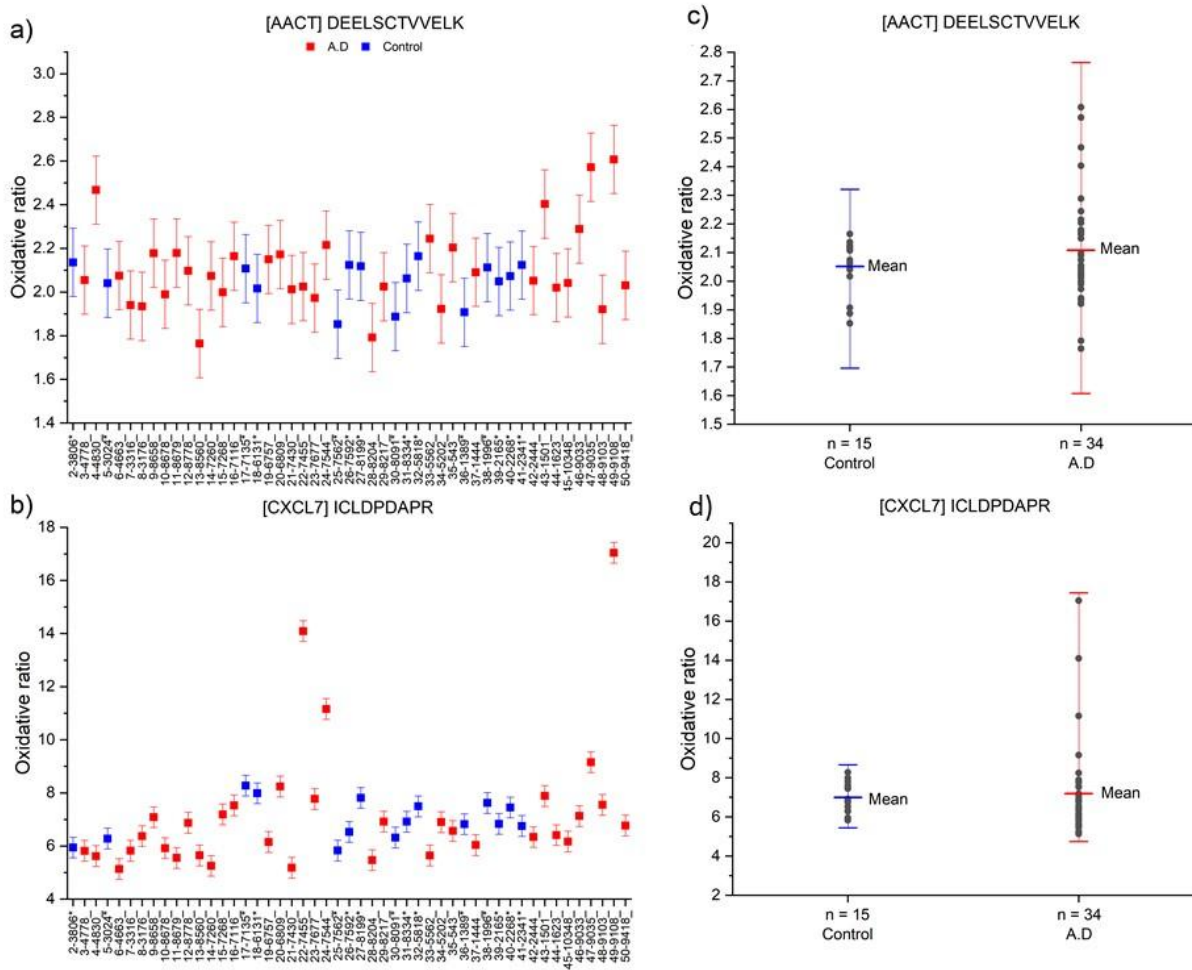


Figure 5: Oxidative ratios of peptides a) DEELSVTVELK [AACT] and b) ICLDPDAPR [CXCL7] in the 49 cohort samples with AD (red) and control (blue) patients. Dispersion of oxidative ratios and means values measured in healthy control group (blue) and AD cohort (red) for c) DEELSVTVELK [AACT] and d) ICLDPDAPR [CXCL7] peptides. The error bars correspond to the standard deviation for each peptide, calculated from the analysis of QC samples.

The oxidative ratios determined from the control (blue) and AD (red) samples are plotted in Figure 5c, d) for respectively DEELSVTVELK [AACT] and ICLDPDAPR [CXCL7] peptides. A

large dispersion of oxidative ratios can be observed in the population with Alzheimer's disease for the DEELSCTVVELK [AACT] and ICLDPDAPR [CXCL7] peptides Figure 5d), e), as expected. In order to assess a potential significant difference between the control and AD samples, peptide oxidative ratios were averaged for all samples within a same group (i.e. mean values). Such as for the other peptides, the mean oxidative ratios of DEELSCTVVELK [AACT] and ICLDPDAPR [CXCL7] were similar between the two populations.

An analysis of variance (ANOVA) was performed in order to check any statistically significant difference between the mean oxidation ratios of the two groups for each peptides. In addition to the quantification at the peptide level, total oxidative ratios per proteins were calculated by averaging the different peptides of each protein within the same sample. Oxidative ratios obtained from the control and AD samples and the ANOVA results, i.e. *p* values, for the 69 peptides are presented in Table S4, while Table 1 summarizes those values for each protein, for better clarity.

Table 1: Oxidative ratio (mean \pm standard deviation) as a function of the protein in healthy controls and diagnosed AD patients

Protein	Group	Oxidative ratio (mean \pm S.D.)	<i>p</i> value
A2MG	Control n = 15	1.167 \pm 0.067	0.165
	AD n = 34	1.134 \pm 0.078	
AACT	Control n = 15	2.051 \pm 0.097	0.285
	AD n = 34	2.108 \pm 0.191	
APOB	Control n = 15	0.984 \pm 0.110	0.199
	AD n = 34	0.947 \pm 0.084	
APOE	Control n = 15	12.347 \pm 3.139	0.615
	AD n = 34	12.787 \pm 2.507	
CERU	Control n = 15	2.822 \pm 0.163	0.302
	AD n = 34	2.759 \pm 0.208	
CFAH	Control n = 15	6.89 \pm 0.516	0.109

	AD n = 34	6.561 ± 0.710	
CO3	Control n = 15	2.542 ± 0.154	0.321
	AD n = 34	2.487 ± 0.187	
CO4A/B	Control n = 15	4.571 ± 0.367	0.488
	AD n = 34	4.469 ± 0.508	
CXLC7	Control n = 15	6.991 ± 0.751	0.766
	AD n = 34	7.188 ± 2.481	
FETUA	Control n = 15	0.200 ± 0.013	0.157
	AD n = 34	0.202 ± 0.019	
FIBA	Control n = 15	0.293 ± 0.024	0.174
	AD n = 34	0.298 ± 0.048	
FIBB	Control n = 15	8.333 ± 0.564	0.780
	AD n = 34	8.269 ± 0.801	
FIBG	Control n = 15	5.280 ± 0.439	0.024
	AD n = 34	4.762 ± 0.533	
FINC	Control n = 15	5.616 ± 0.809	0.233
	AD n = 34	5.302 ± 0.850	
HEMO	Control n = 15	3.448 ± 0.175	0.328
	AD n = 34	3.361 ± 0.322	
HPT	Control n = 15	3.096 ± 0.257	0.865
	AD n = 34	3.079 ± 0.325	
HSA	Control n = 15	2.942 ± 0.174	0.140
	AD n = 34	2.862 ± 0.172	
TransfH	Control n = 15	1.289 ± 0.055	0.498
	AD n = 34	1.333 ± 0.089	
IGKC	Control n = 15	4.467 ± 0.426	0.786
	AD n = 34	4.503 ± 0.419	

risk $\alpha = 0.05$

As indicated by the p values >0.05 , the control and AD samples did not differ significantly in terms of oxidative ratios for 17 of the 19 proteins. In contrast, the analysis of variances of the total oxidative ratio of the DCQDIANK [FIBG] peptide yielded a p value of 0.024, indicating that the inter-population difference is statistically significant. This conclusion is not intuitive in view of the oxidative ratio plots obtained for the control and AD samples (Figure S2d), showing a large dispersion in-between each group. Moreover, the oxidative ratio of DCQDIANK [FIBG] (Figure S2c) exhibited a large standard deviation. The same

observation can be made for the VTAAPQSVCALR [A2MG] peptide (Figure S2a and b), which presented a p value of 0.0052 (Table S4). It is therefore difficult to conclude on the actual difference of DCQDIANK [FIBG] and VTAAPQSVCALR [A2MG] oxidation levels between control and AD populations. The analysis of more AD and control plasma samples would allow to clarify these results and validate putative biomarkers.

If no hint for potential biomarkers of Alzheimer's disease can be extracted from the analysis of the plasmas of the cohort, the developed PRM-LID method allowed to highlight variations in the oxidative levels of proteins. Such direct detection is possible thanks to the specific fragmentation of derivatized endogenous Cys-SOH and Cys-SH peptides in LID, which allows to reduce interfering signal. An even increased sensibility could be obtained using a nano flow configuration. The unbiased relative quantification of protein oxidative ratios with the high multiplexing capacity offered by the PRM can be used for validation of putative biomarkers in large cohorts without sample fractionation or enrichment.

Conclusions

This work presents the development of a PRM-LID methodology for a specific detection and multiplexed relative quantification of low concentrated Cys-SOH plasma proteins from a cohort of AD patients and healthy controls. In order to improve the detection specificity toward the oxidized proteins, we substituted the classical CID mode by LID at 473 nm in order to add an optical specificity to the mass selectivity. Since peptides do not naturally absorb in the visible range, this novel methodological approach relies on the proper chemical derivatization of Cys-SOH proteins with a specific Dabcyl cyclohexanedione chromophore. As a result, only the subset of derivatized peptides are specifically fragmented

in LID, thereby improving the consistency of oxidized protein quantification in biological samples. In order to overcome analytical bias related to sample preparation as well as interpatient variability in the protein expression levels, non-oxidized Cys-SH peptides were derivatized with a Dabcyl maleimide chromophore and used as internal reference. This differential labelling approach allowed to calculate an oxidative ratio by normalizing the signal of each endogenous derivatized Cys-SOH peptide by the signal of the analogue derivatized Cys-SH peptide. 49 plasma samples from a cohort of healthy control and AD patients were sequentially derivatized and then analyzed in targeted PRM-LID, without any enrichment step. CVs of oxidative ratios below 20% for all the targeted peptides were calculated from the statistical analysis of the 12 QCs, showing the robustness of the method. Among the 73 derivatized Cys-SOH/Cys-SH pairs of peptides that were monitored in the study, some variations in the oxidative ratios of AD samples were observed for two peptides related to proteins AACT and CXCL7. However, these variations were not reproduced for all samples and ANOVA statistical analysis of the oxidative ratios between the control and AD populations showed that these variations were not statistically significant (p value >0.05). Laser induced dissociation mass spectrometry with differential tagging nevertheless allows a sensitive, robust, unbiased detection and relative quantification of low concentrated endogenous Cys-SOH proteins, suitable for the analysis of large cohorts of complex biological samples.

Supplementary Material

The Supplementary Material is available free of charge on the website:

Workflow of the sample preparation and chromophore structures, other peptide oxidative ratios, PRM precursor list, analytical performance levels (mean oxidative ratios and CV) from the analysis of 12 QC samples, oxidative ratios and *p* values between the 2 groups for all peptides and URL links to access top10 data sets.

Accession Codes

PRM-LID data are available via PeptideAtlas (<http://www.peptideatlas.org/PASS/PASS01767>).

Links to access the top10 results are provided in the Supplementary Material.

Acknowledgments

The research leading to these results received funding from the French Agence National de la Recherche (ANR) under the Grant Agreement ANR-18-CE29-0002-01 research project “HyLOxi”.

References

- [1] M. Weng, X. Xie, C. Liu, K.L. Lim, C.W. Zhang, L. Li, The Sources of Reactive Oxygen Species and Its Possible Role in the Pathogenesis of Parkinson’s Disease, *Parkinson’s Disease*. 2018 (2018). <https://doi.org/10.1155/2018/9163040>.
- [2] M. Schrag, C. Mueller, M. Zabel, A. Crofton, W.M. Kirsch, O. Ghribi, R. Squitti, G. Perry, Oxidative stress in blood in Alzheimer’s disease and mild cognitive impairment: A meta-analysis, *Neurobiology of Disease*. 59 (2013) 100–110. <https://doi.org/10.1016/j.nbd.2013.07.005>.
- [3] P. Poprac, K. Jomova, M. Simunkova, V. Kollar, C.J. Rhodes, M. Valko, Targeting Free Radicals in Oxidative Stress-Related Human Diseases, *Trends in Pharmacological Sciences*. 38 (2017) 592–607. <https://doi.org/10.1016/j.tips.2017.04.005>.
- [4] G. Aliev, M.A. Smith, D. Seyidova, M.L. Neal, B.T. Lamb, A. Nunomura, E.K. Gasimov, H. v. Vinters, G. Perry, J.C. Lamanna, R.P. Friedland, The role of oxidative stress in the pathophysiology of cerebrovascular lesions in Alzheimer’s disease, *Brain Pathology*. 12 (2002) 21–35. <https://doi.org/10.1111/j.1750-3639.2002.tb00419.x>.

- [5] A.P. Mazzetti, M.C. Fiorile, A. Primavera, M. lo Bello, Glutathione transferases and neurodegenerative diseases, *Neurochemistry International*. 82 (2015) 10–18. <https://doi.org/10.1016/j.neuint.2015.01.008>.
- [6] C.E. Paulsen, K.S. Carroll, Cysteine-mediated redox signaling: Chemistry, biology, and tools for discovery, *Chemical Reviews*. 113 (2013) 4633–4679. <https://doi.org/10.1021/cr300163e>.
- [7] L. Gu, R.A.S. Robinson, Proteomic approaches to quantify cysteine reversible modifications in aging and neurodegenerative diseases, *Proteomics - Clinical Applications*. 10 (2016) 1159–1177. <https://doi.org/10.1002/prca.201600015>.
- [8] J. Yang, K.S. Carroll, D.C. Liebler, The expanding landscape of the thiol redox proteome, *Molecular and Cellular Proteomics*. 15 (2016) 1–11. <https://doi.org/10.1074/mcp.O115.056051>.
- [9] P. Eaton, Protein thiol oxidation in health and disease: Techniques for measuring disulfides and related modifications in complex protein mixtures, *Free Radical Biology and Medicine*. 40 (2006) 1889–1899. <https://doi.org/10.1016/j.freeradbiomed.2005.12.037>.
- [10] Y. Wang, J. Yang, J. Yi, Redox Sensing by Proteins: Oxidative Modifications on Cysteines and the Consequent Events, *Antioxidants & Redox Signaling*. 16 (2012) 649–657.
- [11] N.O. Devarie-Baez, E.I.S. Lopez, C.M. Furdui, Biological chemistry and functionality of protein sulfenic acids and related thiol modifications, *Free Radical Research*. 50 (2016) 172–194. <https://doi.org/10.3109/10715762.2015.1090571>.
- [12] S.E. Leonard, K.S. Carroll, Chemical “omics” approaches for understanding protein cysteine oxidation in biology, *Current Opinion in Chemical Biology*. 15 (2011) 88–102. <https://doi.org/10.1016/j.cbpa.2010.11.012>.
- [13] C.M. Furdui, L.B. Poole, Chemical approaches to detect and analyze protein sulfenic acids, *Mass Spectrometry Reviews*. 33 (2014) 126–146.
- [14] S. Ratnayake, I.H.K. Dias, E. Lattman, H.R. Griffiths, Stabilising cysteinyl thiol oxidation and nitrosation for proteomic analysis, *Journal of Proteomics*. 92 (2013) 160–170. <https://doi.org/10.1016/j.jprot.2013.06.019>.
- [15] G. Chiappetta, S. Ndiaye, A. Igbaria, C. Kumar, J. Vinh, M.B. Toledano, *Proteome screens for Cys residues oxidation: the redoxome.*, 1st ed., Elsevier Inc., 2010. [https://doi.org/10.1016/s0076-6879\(10\)73010-x](https://doi.org/10.1016/s0076-6879(10)73010-x).
- [16] L.I. Leichert, F. Gehrke, H. v. Gudiseva, T. Blackwell, M. Ilbert, A.K. Walker, J.R. Strahler, P.C. Andrews, U. Jakob, Quantifying changes in the thiol redox proteome upon oxidative stress in vivo, *Proc Natl Acad Sci U S A*. 105 (2008) 8197–8202. <https://doi.org/10.1073/pnas.0707723105>.
- [17] S. Shakir, J. Vinh, G. Chiappetta, Quantitative analysis of the cysteine redoxome by iodoacetyl tandem mass tags, *Analytical and Bioanalytical Chemistry*. 409 (2017) 3821–3830. <https://doi.org/10.1007/s00216-017-0326-6>.
- [18] K. Wojdyla, J. Williamson, P. Roepstorff, A. Rogowska-Wrzesinska, The SNO/SOH TMT strategy for combinatorial analysis of reversible cysteine oxidations, *Journal of Proteomics*. 113 (2015) 415–434. <https://doi.org/10.1016/j.jprot.2014.10.015>.

- [19] Y.H. Seo, K.S. Carroll, Quantification of protein sulfenic acid modifications using isotope-coded dimedone and iododimedone, *Angewandte Chemie - International Edition*. 50 (2011) 1342–1345. <https://doi.org/10.1002/anie.201007175>.
- [20] M.C. Crowe, J.S. Brodbelt, Differentiation of phosphorylated and unphosphorylated peptides by high-performance liquid chromatography-electrospray ionization-infrared multiphoton dissociation in a quadrupole ion trap, *Analytical Chemistry*. 77 (2005) 5726–5734. <https://doi.org/10.1021/ac0509410>.
- [21] A. Agarwal, J.K. Diedrich, R.R. Julian, Direct elucidation of disulfide bond partners using ultraviolet photodissociation mass spectrometry, *Analytical Chemistry*. 83 (2011) 6455–6458. <https://doi.org/10.1021/ac201650v>.
- [22] L. Joly, R. Antoine, M. Broyer, P. Dugourd, J. Lemoine, Specific UV photodissociation of tyrosyl-containing peptides in multistage mass spectrometry, *J Mass Spectrom*. 42 (2007) 818–824. <https://doi.org/10.1002/jms>.
- [23] J.P. O'Brien, J.M. Pruet, J.S. Brodbelt, Chromogenic chemical probe for protein structural characterization via ultraviolet photodissociation mass spectrometry, *Analytical Chemistry*. 85 (2013) 7391–7397. <https://doi.org/10.1021/ac401305f>.
- [24] J.K. Diedrich, R.R. Julian, Site selective fragmentation of peptides and proteins at quinone modified cysteine residues investigated by ESI-MS, *Anal Chem*. 82 (2011) 4006–4014. <https://doi.org/10.1021/ac902786q>.Site.
- [25] V.C. Cotham, Y. Wine, J.S. Brodbelt, Selective 351 nm photodissociation of cysteine-containing peptides for discrimination of antigen-binding regions of IgG fragments in bottom-Up liquid chromatography-tandem mass spectrometry workflows, *Analytical Chemistry*. 85 (2013) 5577–5585. <https://doi.org/10.1021/ac400851x>.
- [26] Q. Enjalbert, M. Girod, R. Simon, J. Jeudy, F. Chirot, A. Salvador, R. Antoine, P. Dugourd, J. Lemoine, Improved detection specificity for plasma proteins by targeting cysteine-containing peptides with photo-SRM, *Analytical and Bioanalytical Chemistry*. 405 (2013) 2321–2331. <https://doi.org/10.1007/s00216-012-6603-5>.
- [27] L. Garcia, M. Girod, M. Rompais, P. Dugourd, C. Carapito, J. Lemoine, Data-Independent Acquisition Coupled to Visible Laser-Induced Dissociation at 473 nm (DIA-LID) for Peptide-Centric Specific Analysis of Cysteine-Containing Peptide Subset, *Analytical Chemistry*. 90 (2018) 3928–3935. <https://doi.org/10.1021/acs.analchem.7b04821>.
- [28] M. Girod, J. Biarc, Q. Enjalbert, A. Salvador, R. Antoine, P. Dugourd, J. Lemoine, Implementing visible 473 nm photodissociation in a Q-Exactive mass spectrometer: towards specific detection of cysteine-containing peptides, *Analyst*. 139 (2014) 5523–5530. <https://doi.org/10.1039/C4AN00956H>.
- [29] J.V. Guillaubez, D. Pitrat, Y. Bretonnière, J. Lemoine, M. Girod, Unbiased Detection of Cysteine Sulfenic Acid by 473 nm Photodissociation Mass Spectrometry: Toward Facile in Vivo Oxidative Status of Plasma Proteins, *Analytical Chemistry*. 93 (2021) 2907–2915. <https://doi.org/10.1021/acs.analchem.0c04484>.
- [30] B. MacLean, D.M. Tomazela, N. Shulman, M. Chambers, G.L. Finney, B. Frewen, R. Kern, D.L. Tabb, D.C. Liebner, M.J. MacCoss, Skyline: An open source document editor for creating and

- analyzing targeted proteomics experiments, *Bioinformatics*. 26 (2010) 966–968. <https://doi.org/10.1093/bioinformatics/btq054>.
- [31] R.J. Chalkley, P.R. Baker, K.F. Medzihardszky, A.J. Lynn, A.L. Burlingame, In-depth analysis of tandem mass spectrometry data from disparate instrument types, *Molecular and Cellular Proteomics*. 7 (2008) 2386–2398. <https://doi.org/10.1074/mcp.M800021-MCP200>.
 - [32] A.C. Peterson, J.D. Russell, D.J. Bailey, M.S. Westphall, J.J. Coon, Parallel reaction monitoring for high resolution and high mass accuracy quantitative, targeted proteomics, *Molecular and Cellular Proteomics*. 11 (2012) 1475–1488. <https://doi.org/10.1074/mcp.O112.020131>.
 - [33] G.E. Ronsein, N. Pamir, P.D. von Haller, D.S. Kim, M.N. Oda, G.P. Jarvik, T. Vaisar, J.W. Heinecke, Parallel reaction monitoring (PRM) and selected reaction monitoring (SRM) exhibit comparable linearity, dynamic range and precision for targeted quantitative HDL proteomics, *Journal of Proteomics*. 113 (2015) 388–399. <https://doi.org/10.1016/j.jprot.2014.10.017>.
 - [34] N. Rauniyar, Parallel reaction monitoring: A targeted experiment performed using high resolution and high mass accuracy mass spectrometry, *International Journal of Molecular Sciences*. 16 (2015) 28566–28581. <https://doi.org/10.3390/ijms161226120>.
 - [35] L. Garcia, J. Lemoine, P. Dugourd, M. Girod, Fragmentation patterns of chromophore-tagged peptides in visible laser induced dissociation, *Rapid Communications in Mass Spectrometry*. 31 (2017) 1985–1992. <https://doi.org/10.1002/rcm.7984>.
 - [36] D.M. Hatters, C.A. Peters-Libeu, K.H. Weisgraber, Apolipoprotein E structure: insights into function, *Trends in Biochemical Sciences*. 31 (2006) 445–454. <https://doi.org/10.1016/j.tibs.2006.06.008>.
 - [37] K. Taddei, R. Clarnette, S.E. Gandy, R.N. Martins, Increased plasma apolipoprotein E (apoE) levels in Alzheimer's disease, *Neuroscience Letters*. 223 (1997) 29–32.
 - [38] C. Gabay, C. Kushner, Acute-Phase Proteins and other Systemic Responses to Inflammation, *New England Journal of Medicine*. 340 (1999) 448–454.
 - [39] A.J. Sandford, T. Chagani, T.D. Weir, P.D. Pare, A1-Antichymotrypsin mutations in patients with chronic obstructive pulmonary disease, *Disease Markers*. 13 (1998) 257–260.
 - [40] J. Padmanabhan, M. Levy, D.W. Dickson, H. Potter, Alpha1-antichymotrypsin, an inflammatory protein overexpressed in Alzheimer's disease brain, induces tau phosphorylation in neurons, *Brain*. 129 (2006) 3020–3034. <https://doi.org/10.1093/brain/awl255>.
 - [41] E. Tyagi, T. Fiorelli, M. Norden, J. Padmanabhan, Alpha 1-antichymotrypsin, an inflammatory protein overexpressed in the brains of patients with Alzheimer's disease, induces Tau hyperphosphorylation through c-Jun N-terminal kinase activation, *International Journal of Alzheimer's Disease*. 2013 (2013). <https://doi.org/10.1155/2013/606083>.
 - [42] P.M. Murphy, Chemokines and chemokine receptors, in: *Clinical Immunology*, Elsevier Ltd, 2008: pp. 173–196. <https://doi.org/10.1016/B978-0-323-04404-2.10011-9>.